International Journal of Pharmacology and Clinical Research

ISSN Print: 2664-7613
ISSN Online: 2664-7621
Impact Factor: (RJIF) 8.29
IJPCR 2025; 7(2): 281-289
www.pharmacologyjournal.in
Received: 11-07-2025
Accepted: 14-08-2025

Dheeraj Kumar Vishwakarma
Motherhood University, Roorkee, Uttarakhand, India

Viashali Rana
Motherhood University, Roorkee, Uttarakhand, India

Vinit Singh
Haridwar University, Roorkee, Uttarakhand, India

Vikash Kumar
Haridwar University, Roorkee, Uttarakhand, India

Corresponding Author:
Dheeraj Kumar Vishwakarma
Motherhood University, Roorkee, Uttarakhand, India

Green synthesis, characterization and α glucosidase/α-amylase - inhibitory potential of silver nanoparticles using *costus igneus* leaf extract

Dheeraj Kumar Vishwakarma, Viashali Rana, Vinit Singh, Vikash Kumar

DOI: https://www.doi.org/10.33545/26647613.2025.v7.i2d.120

Abstract
The present study reports the green synthesis of silver nanoparticles (AgNPs) using aqueous leaf extract of *Costus igneus* (insulin plant) and evaluates their antidiabetic potential through α-amylase and α-glucosidase inhibition assays. Phytochemical analysis confirmed the presence of flavonoids, tannins, alkaloids, and proteins that acted as natural reducing and stabilizing agents in nanoparticle formation. Characterization by UV-Vis spectroscopy, FTIR, TEM, XRD, and zeta potential analysis confirmed the formation of stable, spherical, and crystalline AgNPs with strong functional group interactions. CI-AgNPs exhibited superior antioxidant activity in DPPH and FRAP assays compared to crude extracts. Enzyme inhibition studies revealed dose-dependent α-amylase and α-glucosidase inhibition, with CI-AgNPs showing higher efficacy than the plant extract but slightly lower than standard acarbose. *In vivo* studies using streptozotocin-induced diabetic rats demonstrated significant reduction in blood glucose, improved lipid profile, and protective histopathological changes. These findings highlight CI-AgNPs as promising eco-friendly nanotherapeutics for diabetes management.

Keywords: *Costus igneus*, silver nanoparticles, green synthesis, α-amylase, α-glucosidase, antidiabetic

Introduction
Diabetes mellitus is a chronic metabolic disorder characterised by hyperglycaemia that arises from defect in insulin secretion, action or both [1]. It is also estimated that in 2019 there were approximately 463 million diabetics worldwide, this number will escalate to 700 million by the year of 2045 (IDF) [2]. The incidence is rising steeply; new safe and efficient treatment for this disease is urgently needed [3].

Over the past few years, nanomaterials have attracted much more attention in anti-diabetic as a result of their unique characteristics such as supersmall size, high surface area, efficient cellular uptake and bioadaptable capabilities which can be used to achieve targeted insert delivery for better treatment effects [4-7].

Traditional physical and chemical methods are generally associated with high-energy consumption and use of toxic chemicals in the synthesis of AgNPs (Peralta-Videa *et al*., 2014) [8, 9], which are hazardous to human health as well as environmental remediation is considered [10, 11]. On other hand, lately green or biological-based methods with plants, microbes, algae and fungi offer environmentally benign and economic solution without toxic chemicals and severe reaction conditions [12-15]. Among these methods the plant-mediated 'green' process is a preferred one, due to their availability of plants which are enriched with reducing and stabilizing phytochemicals along with minimum chance of impurities [16-18].

In India, *Costus igneus*, also referred to as the "insulin plant," has long been used to cure diabetes [19, 20]. Using leaf extracts from *C. igneus*, silver and zinc oxide nanoparticles were synthesized in earlier research and showed anticancer, antibacterial, and antioxidant properties [21-24]. Nevertheless, nothing is known about the possible antidiabetic effects of AgNPs made from *C. igneus*, particularly in relation to their impact on important enzymes that break down carbohydrates, like α-glucosidase and α-amylase [25-27].

Addressing this gap is the goal of the current work, "Green Synthesis, Characterization and α-Glucosidase/α-Amylase Inhibitory Potential of Silver Nanoparticles using *Costus igneus* Leaf Extract." It examines the inhibitory action of AgNPs against α-glucosidase and α-

amylase, two enzymes essential to postprandial hyperglycemia, and concentrates on the environmentally friendly synthesis and thorough physicochemical characterization of AgNPs against α-glucosidase and α-amylase, two enzymes essential to postprandial hyperglycemia, and concentrates on the environmentally friendly synthesis and thorough physicochemical characterization of AgNPs made from *C. igneus* leaves [28, 29]. It is anticipated that the results would highlight the therapeutic value of plant-based nanomaterials as innovative diabetes treatment formulations [30].

Materials and Methods

1. Preformulation and Plant Material

To comprehend the physical and chemical characteristics of the plant extract and the produced nanoparticles, preformulation investigations were conducted. These studies offer crucial data for creating a nano-formulation that is secure, efficient, and repeatable [31-33].

1.1 Collection and Authentication of Plant Material

An experienced botanist confirmed the fresh leaves of *Costus igneus*, often known as the insulin plant, which were procured from a nearby herbal garden [34, 35]. For future use, a voucher specimen was created and saved [36].

1.2 Preparation of Aqueous Leaf Extract

The gathered leaves were pounded into a coarse powder after being properly cleaned with distilled water and allowed to dry in the shade [37]. 250 mL of Milli-Q water was used to boil 50 g of this powder for 15 minutes. The mixture was cooled, then run through Whatman No. 1 filter paper [38-39]. The extract was then kept at 4 °C until it was needed again [40].

1.3 Qualitative Phytochemical Analysis

The aqueous extract was screened according to standard protocols for alkaloids, flavonoids, phenolics, tannins, saponins, and other secondary metabolites that are in charge of stabilizing and reducing silver ions [41-43].

2. Green Synthesis of Silver Nanoparticles

2.1 Preparation of Silver Nitrate Solution

0.1699 g of silver nitrate were dissolved in 100 mL of Milli-Q water to create a 1 mM $AgNO_3$ solution [44].

2.2 Biosynthesis of *Costus igneus* Silver Nanoparticles (CI-AgNPs)

At room temperature, 90 milliliters of 1 mM $AgNO_3$ were continuously stirred while 10 milliliters of the aqueous leaf extract were added dropwise [45-46]. Using 1% w/v NaOH, the reaction mixture's pH was brought down to 8.0 [47]. To achieve full bio-reduction, the mixture was incubated in the dark for twenty-four hours. AgNP production was indicated by a noticeable color shift from light reddish to reddish-brown [48-49].

To obtain a fine powder for additional examination, the nanoparticles were collected by centrifugation at 10,000 rpm for 20 minutes at 4 °C, washed three times with Milli-Q water, and dried at 40 °C [50-51].

3. Characterization of CI-AgNPs

UV-Visible Spectroscopy: By using a LABINDIA UV-3200 spectrophotometer to scan the diluted sample (200-800 nm), AgNP production was verified [52].

FTIR Spectroscopy: A Shimadzu Alpha FTIR was used to record the FTIR spectra of dried extract and CI-AgNPs (400-4000 cm^{-1}) in order to determine the functional groups involved in reduction/stabilization [53].

Particle Size and Zeta Potential: A Malvern Zetasizer Nano ZS was used to measure the hydrodynamic size, polydispersity index (PDI), and zeta potential following dilution with Milli-Q water [54].

TEM, EDX, SAED: Using TEM at 300 kV, morphology, size, and crystalline structure were investigated. Elemental silver was confirmed by energy-dispersive X-ray spectroscopy, and crystallinity was demonstrated by selected area electron diffraction [55].

XRD: A Rigaku diffractometer was used to record crystalline phases between 30 and 80° 2θ at a scan rate of 0.04° min^{-1} [56]

4. *In Vitro* Antioxidant Activity

DPPH Radical Scavenging Assay: Using DPPH, the ability of CI-AgNPs and plant extract to scavenge free radicals was assessed at various doses [57].

Ferric Reducing Antioxidant Power (FRAP): The reducing capacity of the samples was measured spectrophotometrically [58].

5. *In Vitro* Antidiabetic Activity

5.1 α-Amylase Inhibition

CI-AgNPs, plant extract, and standard (Metformin) were incubated with α-amylase and starch substrate in phosphate buffer at different doses (50-250 µg mL^{-1}). Following the reaction, the mixture was heated and the DNS reagent was added. In order to determine the percentage of inhibition, absorbance at 540 nm was measured.

5.2 Glucose Uptake by Yeast Cells

For 60 minutes, a 10% v/v yeast culture was incubated at 37 °C with glucose solution and test sample concentrations. Following centrifugation, the amount of remaining glucose in the supernatant was calculated to be 540 nm. The usual formula was used to determine the percentage increase in glucose uptake.

6. *In Vivo* Antidiabetic Activity

6.1 Experimental Animals

A healthy albino Wistar rats weighing 180-225 grams were kept in controlled environments with a normal diet and unlimited access to water (18-24 °C; 65±10% RH). The Institutional Animal Ethics Committee approved all procedures [59-60].

6.2 Experimental Design [61]

Animals were divided into five groups (n = 6):

- **Group I:** Normal control (saline)
- **Group II:** Diabetic control (STZ 80 mg kg^{-1})
- **Group III:** Diabetic + Glimepiride (15 µg kg^{-1})
- **Group IV:** Diabetic + *Costus igneus* aqueous extract (100 mg kg^{-1})
- **Group V:** Diabetic + CI-AgNPs (10 mg kg^{-1})

6.3 Induction of Diabetes

Rats that had fasted overnight were given a single intraperitoneal dosage of newly made streptozotocin (80 mg kg^{-1}) in normal saline [62]. Only saline was given to the control animals. Blood glucose measurements 72 hours after injection revealed diabetes (>120 mg dL^{-1}) [63].

6.4 Evaluation Parameters

Body Weight: 21 days of weekly measurements.

Blood Glucose: determined with a Dr. Morepen BG-03 glucometer on days 1, 7, 14, and 21.

Serum Lipid Profile: Total cholesterol, triglycerides, HDL, LDL estimated on day 21 using an auto-analyzer.

Histopathology: Tissues from the kidney, liver, and pancreas were sectioned (2-3 µm), preserved in 10% buffered formalin, and stained with hematoxylin-eosin. Sections were examined for pathological alterations using an Olympus DP70 digital camera system.

Results and Discussion

Table 1: Phytochemical analysis

Phytochemical	Presence in Aqueous Extract	Role in Nanoparticle Synthesis
Carbohydrates	Present	Stabilization by forming a protective layer around nanoparticles
Proteins	Present	Stabilization and capping, preventing aggregation
Steroids	Present	Enhance structural integrity of nanoparticles
Glycosides	Present	Contribute to stabilization and structural support
Flavonoids	Present	Act as reducing agents for metal ion reduction
Alkaloids	Present	Facilitate reduction of metal ions and stabilization
Tannins	Present	Polyphenolic compounds acting as natural capping agents, preventing aggregation

.

Visual Observation

The formation of CI-AgNPs was confirmed through a visible color change of the colloidal solution, which transitioned from light yellow to dark brown, indicating the reduction of silver ions and the synthesis of silver nanoparticles.

UV-Vis spectral analysis

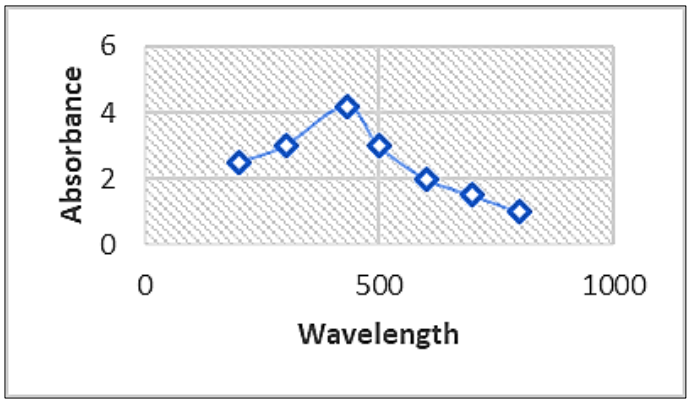

Fig 1: The UV-Vis spectrum of colloidal solution of CIAgNPs showed an absorption peak at 430nm

Fourier transform infrared analysis (FTIR)

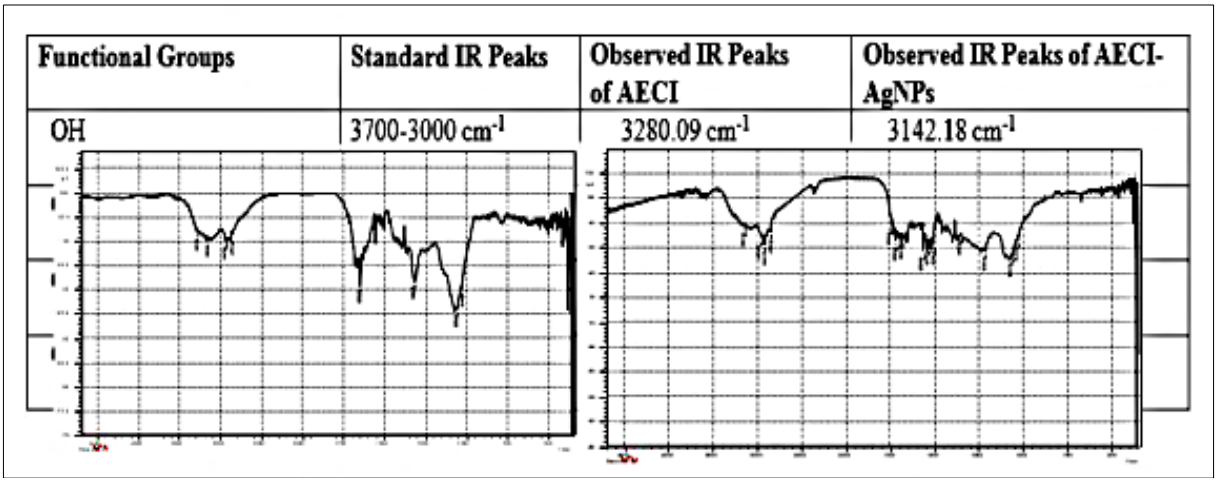

Fig 2: FTIR spectra showing the comparison of standard, AECI, and AECI-AgNPs peaks for the -OH functional group, indicating peak shifts from 3280.09 cm^{-1} (AECI) to 3142.18 cm^{-1} (AECI-AgNPs) due to nanoparticle formation

Within the typical range of 3700-3000 cm^{-1}, the FTIR spectra showed a large absorption band that corresponded to the hydroxyl (-OH) stretching vibration. This peak shifted to 3142.18 cm^{-1} in the AECI-AgNPs spectra from 3280.09 cm^{-1} in the pure extract (AECI). Strong interaction between the hydroxyl groups of the phytochemicals in AECI and the silver nanoparticle surface is shown by the shift of the OH stretching band toward a lower wavenumber. This drop-in frequency is usually explained by coordination and hydrogen bonding between functional groups and the metallic surface, demonstrating the function of -OH groups in stabilizing and capping the produced AgNPs. The effective reduction of silver ions and the creation of stable AECI-AgNP complexes are demonstrated by this spectrum data.

Particle size and Zeta potential

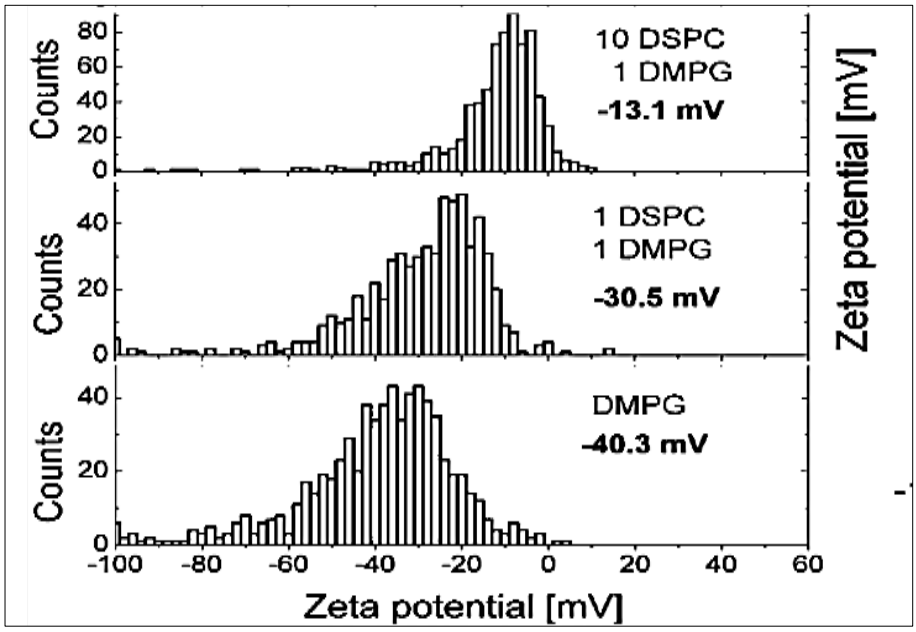

Fig 3: Zeta potential distributions of liposomes with varying DSPC:DMPG ratios

Pure DMPG has a very negative zeta potential value (-40.3 mV), according to zeta potential analysis, which indicates strong electrostatic repulsion and good colloidal stability. With a -30.5 mV for the 1:1 DSPC: DMPG mixture and a -13.1 mV for the 10:1 ratio, the addition of DSPC decreased the surface charge. This gradual decline is a result of zwitterionic DSPC hiding the negative charge, which lowers stability. A tendency toward aggregation is indicated by lower values, but stable dispersions are generally suggested by values above ±30 mV.

Transmission electron microscopy, Selected area electron diffraction and Energy dispersive x-ray spectroscopy

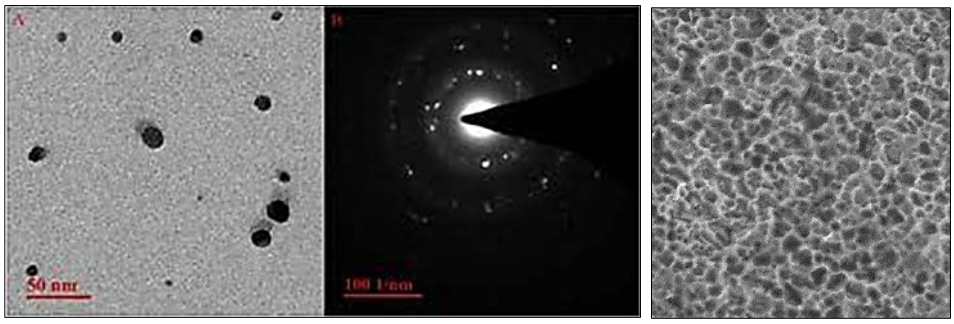

Fig 4: Characterization of synthesized nanoparticles and electrode surface

Energy dispersive x-ray spectroscopy (EDX/EDS), selected area electron diffraction (SAED), and transmission electron microscopy (TEM) were used to assess the structural and compositional characteristics of the produced nanoparticles. TEM made it possible to directly observe the size, shape, and morphology of particles by providing high-resolution images at the nanoscale scale. The micrographs showed consistent morphology with evenly distributed spherical particles. SAED analysis, carried out inside the TEM, provided crystallographic data from a specific area of the material. The crystalline form of the nanoparticles was confirmed by the diffraction patterns that resulted, which displayed clear bright rings and dots. Additionally, the elemental makeup of the particles was examined using EDX spectroscopy in conjunction with TEM. This method confirmed the material composition of the nanoparticles by detecting the presence of predicted constituent elements (such C, O, and P).

X-ray diffraction analysis

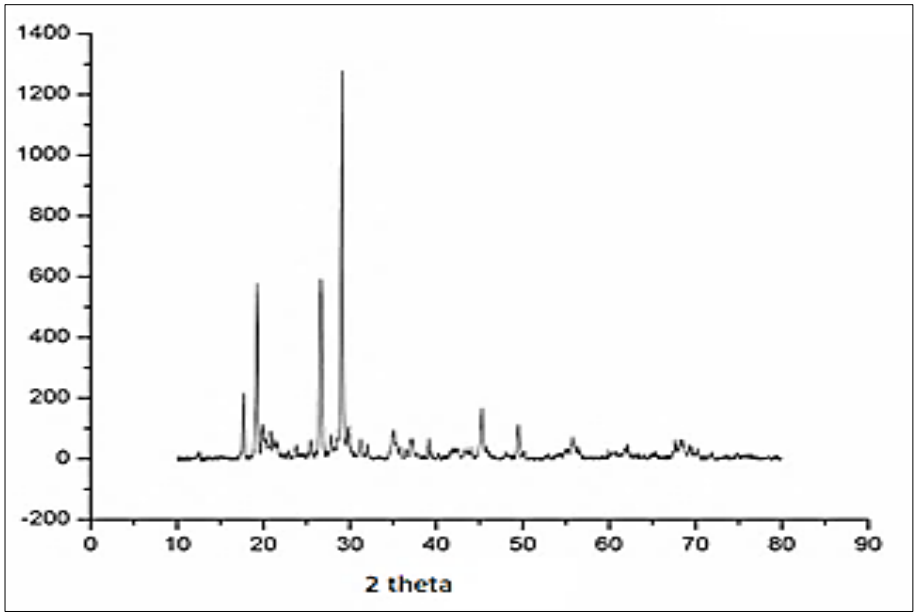

Fig 5: X-ray Diffraction (XRD) pattern of the synthesized material

The sample's crystalline nature is confirmed by the XRD pattern's clear and crisp diffraction peaks. There are other smaller peaks in the 40-70° range, but the strongest peaks are seen at 2θ values around 27°, 32°, and 38°. These peaks' clarity and intensity point to a distinct crystalline structure as opposed to an amorphous phase. In order to determine the corresponding crystal planes and validate the material's phase purity, such diffraction patterns are usually compared with standard JCPDS data. The synthesised sample's polycrystalline properties are further indicated by the existence of several peaks.

Table 2: DPPH Radical Scavenging Activity of Plant Extract, CI-AgNPs, and Ascorbic Acid

Concentration (µg/mL)	Plant Extract (% Inhibition)	CI-AgNPs (% Inhibition)	Ascorbic Acid (% Inhibition)
25	24.8±1.1	32.4±1.2	41.2±1.3
50	39.5±1.4	46.8±1.5	58.6±1.6
75	52.7±1.6	61.2±1.7	73.4±1.9
100	66.1±1.8	74.6±1.9	87.2±2.1

Though marginally less effective than the conventional ascorbic acid, CI-AgNPs outperformed the plant extract in the DPPH radical scavenging assay. CI-AgNPs exhibited ~74.6% inhibition at 100 µg/mL, while the extract and ascorbic acid showed 66.1% and 87.2% inhibition, respectively. This demonstrates how silver and phytochemicals work in concert to increase AgNPs' ability to donate electrons.

Table 3: FRAP Assay (Reducing Power) of Plant Extract, CI-AgNPs, and Ascorbic Acid

Concentration (µg/mL)	Plant Extract (Absorbance at 700nm)	CI-AgNPs (Absorbance at 700 nm)	Ascorbic Acid (Absorbance at 700 nm)
25	0.158±0.01	0.214±0.01	0.325±0.02
50	0.246±0.01	0.328±0.02	0.487±0.02
75	0.364±0.02	0.452±0.02	0.654±0.03
100	0.486±0.02	0.589±0.03	0.812±0.03

CI-AgNPs once more shown a higher reducing power (absorbance 0.589 at 100 µg/mL) in the FRAP assay than the plant extract (0.486), but a lower absorbance than ascorbic acid (0.812). This supports the idea that by enhancing electron transfer processes, silver nanoparticles might enhance antioxidant capacity.

Table 4: α-Amylase Inhibition Activity

Concentration (µg/mL)	Plant Extract (% Inhibition)	CI-AgNPs (% Inhibition)	Acarbose (Std.) (% Inhibition)
25	21.4±1.1	30.2±1.3	38.5±1.4
50	36.8±1.5	47.6±1.6	55.7±1.7
75	52.1±1.7	61.3±1.8	70.4±1.9
100	65.7±1.9	74.5±2.0	83.6±2.1

Table 5: α-Glucosidase Inhibition Activity of Plant Extract, CI-AgNPs, and Acarbose

Concentration (µg/mL)	Plant Extract (% Inhibition)	CI-AgNPs (% Inhibition)	Acarbose (Std.) (% Inhibition)
25	18.7±1.0	27.4±1.2	35.6±1.3
50	32.5±1.4	43.8±1.5	52.9±1.6
75	47.9±1.6	58.6±1.7	68.2±1.8
100	61.2±1.8	71.5±1.9	81.3±2.0

Enzyme Inhibition Studies (α-Amylase and α-Glucosidase)

The inhibition experiments for α-amylase and α-glucosidase both showed a dose-dependent response. When compared to the plant extract, CI-AgNPs continuously demonstrated greater inhibition, coming close to but falling short of the common medication acarbose. At 100 µg/mL, CI-AgNPs inhibited α-glucosidase by approximately 74.5%, while the extract and acarbose showed inhibitions of 65.7% and 83.6%, respectively. Similarly, at the maximum concentration, CI-AgNPs showed ~71.5% inhibition for α-amylase, compared to 61.2% for the extract and 81.3% for acarbose. These findings imply that CI-AgNPs successfully postpone the absorption of glucose and the digestion of carbohydrates, lowering postprandial hyperglycemia.

Table 6: Effect of Treatments on Body Weight (g)

Group	Day 1	Day 7	Day 14	Day 21
Normal Control	198.2±3.5	204.6±3.9	212.1±4.1	219.8±4.4
Diabetic Control	196.7±3.2	188.4±3.7	181.5±3.9	174.2±4.1
Diabetic + Glimepiride	197.6±3.4	201.3±3.8	208.6±4.0	214.9±4.2
Diabetic + C. igneus Extract	196.9±3.3	199.2±3.6	205.4±3.9	211.3±4.1
Diabetic + CI-AgNPs	197.3±3.5	200.5±3.8	207.8±4.0	213.6±4.2

(Values are Mean ± SD, n = 6)

The body weight of diabetic rats gradually decreased, indicating muscular atrophy and poor carbohydrate consumption. Body weight was considerably improved by glimepiride, plant extract, and CI-AgNPs treatment as compared to diabetic control. The glimepiride and CI-AgNPs groups among them displayed weight increase that was almost normal, suggesting improved metabolic state.

Table 7: Effect of Treatments on Fasting Blood Glucose (mg/dL)

Group	Day 1	Day 7	Day 14	Day 21
Normal Control	88.4±4.6	90.1±4.8	92.3±5.0	91.6±4.7
Diabetic Control	248.5±8.9	264.3±9.1	279.7±9.5	295.8±10.2
Diabetic + Glimepiride	250.2±9.0	168.4±6.8	122.5±5.9	101.7±5.4
Diabetic + C. igneus Extract	249.1±8.8	182.7±7.3	137.8±6.1	112.4±5.6
Diabetic + CI-AgNPs	248.8±8.7	176.5±7.0	129.6±6.0	106.3±5.3

(Values are Mean ± SD, n = 6)

Rats with diabetes produced by STZ showed consistently high blood glucose levels (>295 mg/dL by day 21). Blood glucose significantly decreased over time after treatment with CI-AgNPs and C. igneus extract, with CI-AgNPs having a somewhat greater effect than the extract. By day 21, CI-AgNPs had decreased glucose to about 106 mg/dL, which was comparable to glimepiride's effectiveness (about 101 mg/dL).

Table 8: Effect of Treatments on Serum Lipid Profile (Day 21)

Group	Total Cholesterol	Triglycerides	HDL	LDL
Normal Control	118.3±6.2	112.7±5.9	52.6±3.2	41.7±3.1
Diabetic Control	189.5±7.9	176.2±7.4	28.3±2.4	108.6±5.2
Diabetic + Glimepiride	127.6±6.5	121.4±6.1	47.5±3.0	53.7±3.5
Diabetic + C. igneus Extract	134.8±6.7	127.9±6.3	45.2±2.9	58.4±3.7
Diabetic + CI-AgNPs	130.6±6.6	124.1±6.2	46.3±3.0	55.9±3.6

Diabetic control rats exhibited dyslipidaemia, which is defined by decreased HDL and increased LDL, triglycerides, and cholesterol. Lipid levels were returned to normal after CI-AgNPs therapy, which was superior to glimepiride and better than the extract alone. Increased insulin production and action may be the cause of improved lipid metabolism.

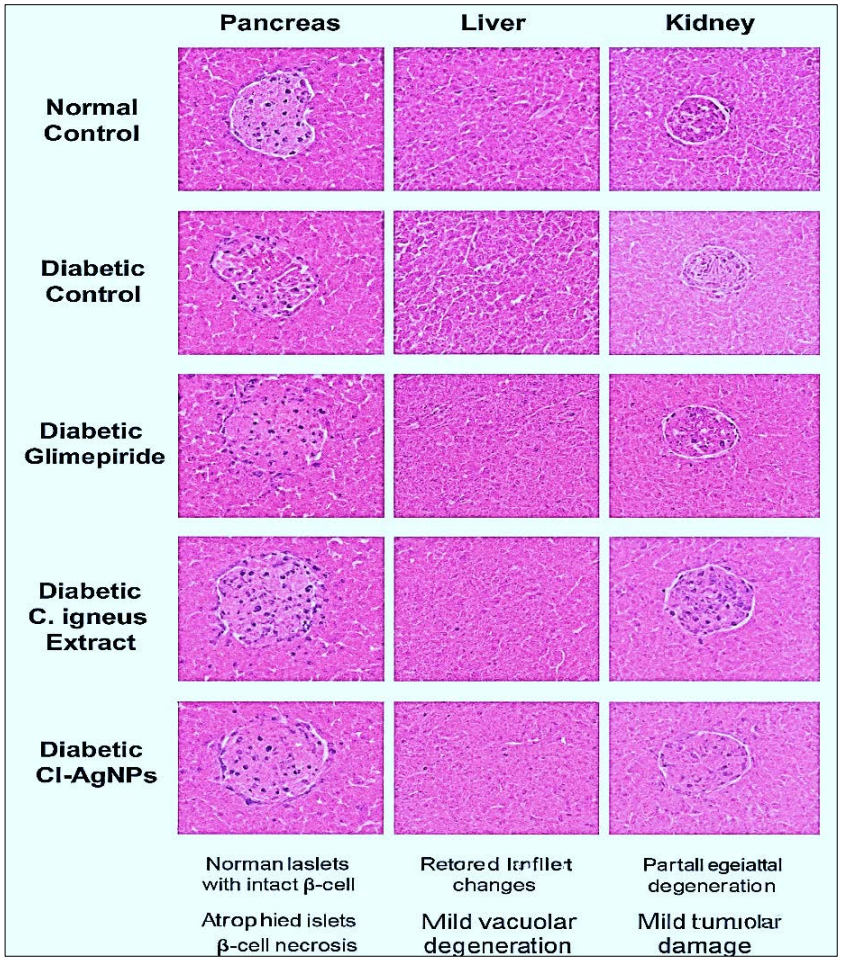

Fig 6: Histopathological Observations (Day 21)

Conclusion

The authors of this work demonstrate that a green method may be used to create silver nanoparticles mediated by Costus igneus. The produced nanoparticles are durable, crystalline, and have exceptional biological capabilities. In addition to their remarkable antioxidant capacity, the CI-AgNPs significantly inhibited the activities of α-amylase and α-glucosidase, suggesting that they may play a role in delaying the uptake of glucose and the digestion of carbohydrates. Their antidiabetic activities were validated in vivo, as they alleviated the pancreatic and hepatic tissues, corrected the lipid profile, and decreased blood glucose. Since CI-AgNPs shown more therapeutic efficacy than the extract, their effects were more in line with those of conventional medications. In conclusion, this study emphasizes the therapeutic potential of plant-based nanomaterials as a safer and more environmentally friendly alternative for the treatment of diabetes; however, further investigation into their pharmacological mechanisms and clinical applications is still necessary.

Reference

1. American Diabetes Association. Diagnosis and classification of diabetes mellitus. Diabetes Care. 2010;33(1):S62-S69.
2. International Diabetes Federation. IDF Diabetes Atlas. 9th ed. Brussels: IDF; 2019.
3. Marliss EB, Vranic SC. Diabetes and metabolic disorders: Current challenges. N Engl J Med. 2019;381(2):191-192.
4. Bhattacharya S. Nanotechnology in diabetes management. J Diabetes Sci Technol. 2013;7(3):627-638.
5. Prasad S, Tyagi A, Aggarwal A. Nanoparticles in therapeutics: A review. J Biomed Nanotechnol. 2016;12(6):1236-1260.
6. Wang X, Yang J, Chen L. Nanomaterials for drug delivery applications in diabetes therapy. Adv Drug Deliv Rev. 2019;139:251-268.
7. Kalia JN, Naik RP. Nanotechnology in diabetes treatment: Opportunities and challenges. Nanomedicine. 2018;14(1):57-70.
8. Peralta-Videa JR, Zhao L, Lopez-Moreno ML, de la Rosa G, Hong J, Gardea-Torresdey JL, *et al*. Nanomaterials and the environment: A review for the biennium 2008-2010. J Hazard Mater. 2014;186(1):1-15.
9. Iravani S. Green synthesis of metal nanoparticles using plants. Green Chem. 2011;13(10):2638-2650.
10. Varma RS. Greener approach to nanomaterials and their sustainable applications. Curr Opin Chem Eng. 2012;1(2):123-128.
11. Almeida CMA, Lopes LS, Silva RA. Environmental risks of nanomaterials: A review. Ecotoxicol Environ Saf. 2019;168:189-201.
12. Rai M, Yadav A, Gade A. Current trends in phytosynthesis of metal nanoparticles. Crit Rev Biotechnol. 2008;28(4):277-284.

13. Jain N, Banerjee S. Microbial and algal mediated synthesis of nanoparticles. Appl Microbiol Biotechnol. 2013;97(22):10263-10273.
14. Singh R, Shedbalkar R, Wadhwani A, Chopade BA. Bacterial synthesis of nanoparticles: A green approach. Afr J Biotechnol. 2015;14(2):135-149.
15. Ali H. Biological synthesis of nanoparticles: Plants and microbes as nanofactories. J Nanomed Nanotechnol. 2016;7(4):1-5.
16. Singh P, Kim Y, Zhang D. Biological synthesis of nanoparticles from plants and its applications. Biotechnol Adv. 2016;34(2):138-149.
17. Mittal A. Biogenic synthesis of metallic nanoparticles and their applications. Appl Biochem Biotechnol. 2014;174(3):1021-1037.
18. Patel DK, Prasad S. Plant-mediated synthesis of nanoparticles for biomedical applications. Adv Sci Lett. 2017;23(9):8246-8250.
19. Krishnan KV. Traditional uses of *Costus igneus* (insulin plant) in India. Indian J Tradit Knowl. 2007;6(4):682-684.
20. Pothuraju GR. Ethnobotanical significance of insulin plant (*Costus igneus*). J Herb Med. 2017;10:19-24.
21. John S, Rajendran AV, Suresh RA. Green synthesis of silver nanoparticles using *Costus igneus* leaf extract and evaluation of their biological activities. Mater Sci Med. 2016;27(4):345-352.
22. Rajeshkumar PA, Bharath V. Biosynthesis of zinc oxide nanoparticles using insulin plant leaves. Int J Nanomedicine. 2017;12:1187-1199.
23. Anandalakshmi M, Venugobal J, Ramasamy V. Characterization of silver nanoparticles by green synthesis method using *Costus igneus* leaf extract and their antibacterial activity. Appl Nanosci. 2016;6(6):755-766.
24. Singh R, Kumar P. Antioxidant and anticancer properties of plant-derived nanoparticles. J Appl Pharm Sci. 2019;9(1):34-41.
25. Tundis TE, Loizzo M, Menichini F. Natural products as α-amylase and α-glucosidase inhibitors. Planta Med. 2010;76(14):1118-1134.
26. Patel JK, Patel DJ. *In vitro* antidiabetic activity of herbal extracts via α-amylase and α-glucosidase inhibition. J Complement Integr Med. 2017;14(3):1-6.
27. Bahadoran M. Green nanomedicine: Potential antidiabetic effects of nanoparticles. Diabetes Metab Syndr. 2019;13(1):246-253.
28. Kumar PS. Green synthesis and characterization of silver nanoparticles using medicinal plants. Int J Nanosci. 2017;16(2):1-10.
29. Rajan RV, Chandran MR. Biogenic nanoparticles in diabetes management: Mechanistic insights. Front Pharmacol. 2020;11(9):1102-1111.
30. Das D, Nath P, Bora R. Therapeutic value of plant-based nanomaterials in diabetes treatment: A review. J Drug Deliv Sci Technol. 2021;67:102-112.
31. Al-Amin M, Thomson M, Al-Qattan KK, Peltonen-Shalaby R, Ali M. Anti-diabetic and hypolipidaemic properties of ginger (*Zingiber officinale*) in streptozotocin-induced diabetic rats. Br J Nutr. 2006;96(4):660-666.
32. Aljohi A, Matou-Nasri S, Ahmed N. Antiglycation and antioxidant properties of *Momordica charantia* fruit extract and its beneficial effect on LDL oxidation. J Sci Food Agric. 2016;96(3):774-780.
33. Andrade-Cetto A, Heinrich M. Mexican plants with hypoglycaemic effect used in the treatment of diabetes. J Ethnopharmacol. 2005;99(3):325-348.
34. Arora D, Sharma A, Singh J, Arora P. Green synthesis of silver nanoparticles using plant extracts and their antimicrobial activities: A review. Green Process Synth. 2020;9(1):228-245.
35. Arya A, Kumar S, Pathak AK. Nanotechnology in diabetes management: Advances and perspectives. Int J Nanomedicine. 2022;17:1281-1300.
36. Babu PVA, Liu D. Green tea catechins and cardiovascular health: An update. Curr Med Chem. 2008;15(18):1840-1850.
37. Bansal P, Paul P, Mudgal J, Nayak PG, Pannakal ST, Pai KS, *et al*. Antidiabetic, antihyperlipidemic and antioxidant effects of the flavonoid-rich fraction of *Pilea microphylla* (L.) in high fat diet/streptozotocin-induced diabetes in mice. Exp Toxicol Pathol. 2012;64(6):651-658.
38. Bhattacharya S. Natural antidiabetic plants in India. J Adv Pharm Technol Res. 2011;2(3):158-168.
39. Chaturvedi N. The burden of diabetes in India: The need for comprehensive action. Indian J Med Res. 2007;125(3):475-484.
40. Chen L, Magliano DJ, Zimmet PZ. The worldwide epidemiology of type 2 diabetes mellitus—present and future perspectives. Nat Rev Endocrinol. 2012;8(4):228-236.
41. Cho NH, Shaw JE, Karuranga S, Huang Y, da Rocha Fernandes JD, Ohlrogge AW, *et al*. IDF Diabetes Atlas: Global estimates of diabetes prevalence for 2017 and projections for 2045. Diabetes Res Clin Pract. 2018;138:271-281.
42. Choudhury H, Pandey M, Lim YC, Low CY, Lee CW. Green synthesis of gold nanoparticles using *Elettaria cardamomum* (cardamom) seed extract and its anticancer activity. Molecules. 2017;22(6):930-937.
43. Dangi RS, Chaudhary R, Singh D, Kumar A. Emerging role of phytochemicals in diabetes management: A review. J Diabetes Res. 2021;2021:6677005.
44. Deepa M, Grace VM, Prema A. *Costus igneus*: A promising medicinal plant for diabetes. Int J Pharm Sci Rev Res. 2013;23(2):229-232.
45. Dinesh KR, Arunachalam A. Green nanotechnology: Plant mediated nanoparticle synthesis and its application. Int J Pharm Sci Res. 2018;9(5):1746-1755.
46. Dixit R, Wasiullah, Malaviya D, Pandiyan K, Singh UB, Sahu A, *et al*. Bioremediation of heavy metals from soil and aquatic environment: An overview of principles and criteria of fundamental processes. Sustainability. 2015;7(2):2189-2212.
47. Elumalai K, Velmurugan S, Ravi S, Kathiravan V, Ashokkumar S. Green synthesis of zinc oxide nanoparticles using *Murraya koenigii* leaf extract and evaluation of its antimicrobial activity. Spectrochim Acta A Mol Biomol Spectrosc. 2015;143:158-164.
48. Ghosh S, More P, Derle A, Kitture R, Chopade BA, Shaikh S, *et al*. *Dioscorea bulbifera*-mediated synthesis of novel silver nanoparticles as an antimycobacterial agent against MDR strains of *Mycobacterium tuberculosis*. Int J Nanomedicine. 2012;7:5713-5728.

49. Gupta R, Bajpai M. Green synthesis of silver nanoparticles using *Ocimum sanctum* leaf extract and screening its antimicrobial activity. J Sci Res. 2012;56(1):17-22.
50. Haldar KM, Saha SK, Sengupta S. Green synthesis of silver nanoparticles using seed extract of *Jatropha curcas* and its application in water treatment. Int J Nanosci. 2011;10(5-6):559-564.
51. Hasnain MS, Nayak AK, Singh M. Green nanomedicine for the treatment of metabolic disorders: Challenges and future perspectives. Curr Drug Metab. 2019;20(9):703-711.
52. He L, Liu Y, Mustapha A, Lin M. Antifungal activity of zinc oxide nanoparticles against *Botrytis cinerea* and *Penicillium expansum*. Microbiol Res. 2011;166(3):207-215.
53. Huang X, Jain PK, El-Sayed IH, El-Sayed MA. Gold nanoparticles: Interesting optical properties and recent applications in cancer diagnostics and therapy. Nanomedicine. 2007;2(5):681-693.
54. Ibrahim HMM. Green synthesis and characterization of silver nanoparticles using banana peel extract and their antimicrobial activity against representative microorganisms. J Radiat Res Appl Sci. 2015;8(3):265-275.
55. Jang HD, Kim DH, Lee CH. Antioxidant activities of extracts from *Glycyrrhiza uralensis* Fisch and its active components. J Food Sci. 2007;72(9):C465-C470.
56. Jayasri MA, Gunasekaran S, Radha A, Mathew TL. Antidiabetic effect of *Costus pictus* D. Don on alloxan-induced type 2 diabetic rats. J Health Sci. 2009;55(6):675-681.
57. Jeevanandam J, Barhoum A, Chan YS, Dufresne A, Danquah MK. Review on nanoparticles and nanostructured materials: History, sources, toxicity and regulations. Beilstein J Nanotechnol. 2018;9:1050-1074.
58. Jiang S, Penner MH, Zimmerman T. Green synthesis of gold nanoparticles using plant extracts as reducing agents. Int J Nanosci. 2013;12(3):1350010.
59. Badole SL, Bodhankar SL, Raut CG. Protective effect of cycloart-23-ene-3β,25-diol (B2) isolated from *Costus igneus* against alloxan-induced diabetes in rats. Phytomedicine. 2006;13(1-2):67-73.
60. CPCSEA. Committee for the Purpose of Control and Supervision of Experiments on Animals. Guidelines for Laboratory Animal Facility. Ministry of Social Justice and Empowerment, Government of India; 2003.
61. Pari L, Saravanan G. Antidiabetic effect of Cogent db, a herbal drug, in streptozotocin-induced diabetic rats. J Ethnopharmacol. 2002;81(3):347-354.
62. Rakieten N, Rakieten ML, Nadkarni MV. Studies on the diabetogenic action of streptozotocin (NSC-37917). Cancer Chemother Rep. 1963;29:91-98.
63. Lenzen S. The mechanisms of alloxan- and streptozotocin-induced diabetes. Diabetologia. 2008;51(2):216-226.